JACS
JOURNAL OF THE AMERICAN CHEMICAL SOCIETY

Subscriber access provided by American Chemical Society

Article

Influence of Alkyl Substituents on the Solution- and Surface-Organization of Hexa-*peri*-hexabenzocoronenes

Marcel Kastler, Wojciech Pisula, Daniel Wasserfallen, Tadeusz Pakula, and Klaus Mllen

J. Am. Chem. Soc., **2005**, 127 (12), 4286-4296• DOI: 10.1021/ja0430696 • Publication Date (Web): 05 March 2005

Downloaded from http://pubs.acs.org on March 24, 2009

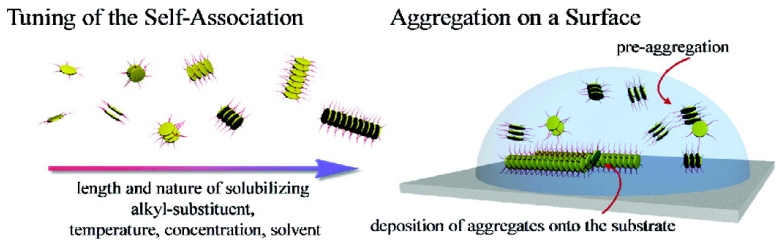

More About This Article

Additional resources and features associated with this article are available within the HTML version:

- Supporting Information
- Links to the 45 articles that cite this article, as of the time of this article download
- Access to high resolution figures
- Links to articles and content related to this article
- Copyright permission to reproduce figures and/or text from this article

View the Full Text HTML

ACS Publications
High quality. High impact.

Journal of the American Chemical Society is published by the American Chemical Society. 1155 Sixteenth Street N.W., Washington, DC 20036

J|A|C|S
ARTICLES
Published on Web 03/05/2005

Influence of Alkyl Substituents on the Solution- and Surface-Organization of Hexa-*peri*-hexabenzocoronenes

Marcel Kastler, Wojciech Pisula, Daniel Wasserfallen, Tadeusz Pakula, and Klaus Müllen*

Contribution from the Max-Planck-Institute for Polymer Research, Postfach 3148, D-55021 Mainz, Germany

Received November 17, 2004; E-mail: muellen@mpip-mainz.mpg.de

Abstract: Three hexa-*peri*-hexabenzocoronenes (HBCs) with branched, bulky alkyl substituents of different lengths in the periphery of the aromatic core have been synthesized to tune the self-association properties in solution. ^{1}H NMR and photophysical measurements were used to probe the solution organization in comparison to the known hexa-dodecyl-substituted HBC in different solvent systems. Thermodynamic parameters for the self-association in solution, obtained by curve fitting of the concentration- and temperature-dependent NMR data using van't Hoff analysis, indicated that the self-association is an enthalpically driven process that is entropically disfavored. Photoluminescence and NMR results were both employed to determine the critical concentration where no self-association for different compounds occurred. The interactions between the molecules could be controlled by varying the nonsolvent content in the solvent mixtures, supporting the model of solvophobic effects. The spatial demand of the solubilizing side chains modulated the self-association in solution. This behavior was translated into the solution casting process, where the kinetic in addition to the thermodynamic parameters played an essential role for structure formation. The study illuminates the relationship between the solution association of HBCs and the morphology, when processed on a surface. These results are essential for the application of these materials in devices.

Introduction

The self-assembly of single elements into complex, organized supramolecular structures via specific intermolecular interactions is impressively illustrated in nature, for example, by the base-pair stacking in the DNA[1] and tertiary structures of proteins. This principle transfers the intrinsic information from the molecular level onto the superstructure.[2] To exploit this concept for material science, it is important to understand the interactions between the single building blocks.[3] Different noncovalent interactions between the molecules play significant roles during the self-assembly. Inspired by nature, the main challenge of supramolecular chemistry is to design specific intermolecular interactions leading to the desired architectures with increased size and complexity. Different attractive intermolecular forces, such as hydrogen bonding,[4] metal coordination, and π-stacking,[5] can dominate individually or cooperate to establish the organization and stability of the system.[6]

A prominent class of such compounds utilizes aromatic stacking to form one-dimensional columnar rods in solution. The electrostatic driving force of these aromatic interactions is the result of an attraction between the positively charged σ-framework and the negatively charged electron cloud of the neighboring units.[7] Moore and co-workers reported the synthesis of various types of shape-persistent phenylacetylene macrocycles (PAMs).[8] They investigated the influence of substitution, temperature, and solvent on the self-association behavior. The solution-phase organization of other macrocycles,[9] helicenes,[10] porphyrins,[11] and phthalocyanines[12] has also been reported.

Discotic liquid crystals have attracted considerable interest due to their self-organization and electronic properties. These

(1) Watson, J. D.; Crick, F. H. C. *Nature* **1953**, *171*, 737−738.
(2) (a) Bong, D. T.; Clark, T. D.; Granja, J. R.; Ghadiri, M. R. *Angew. Chem., Int. Ed.* **2001**, *40*, 988−1011. (b) Percec, V.; Ahn, C. H.; Ungar, G.; Yeardley, D. J. P.; Moller, M.; Sheiko, S. S. *Nature* **1998**, *391*, 161−164.
(3) (a) Brunsveld, L.; Folmer, B. J. B.; Meijer, E. W.; Sijbesma, R. P. *Chem. Rev.* **2001**, *101*, 4071−4097. (b) Ciferri, A. *Makromol. Chem., Rapid Commun.* **2002**, *23*, 511−529.
(4) (a) Prins, L. J.; Reinhoudt, D. N.; Timmerman, P. *Angew. Chem., Int. Ed.* **2001**, *40*, 2383−2426. (b) Sherrington, D. C.; Taskinen, K. A. *Chem. Soc. Rev.* **2001**, *30*, 83−93. (c) Hirschberg, J.; Brunsveld, L.; Ramzi, A.; Vekemans, J.; Sijbesma, R. P.; Meijer, E. W. *Nature* **2000**, *407*, 167−170.
(5) (a) Hunter, C. A.; Lawson, K. R.; Perkins, J.; Urch, C. J. *J. Chem. Soc., Perkin Trans. 2* **2001**, 651−669. (b) Gallivan, J. P.; Schuster, G. B. *J. Org. Chem.* **1995**, *60*, 2423−2429.
(6) (a) van Gorp, J. J.; Vekemans, J.; Meijer, E. W. *J. Am. Chem. Soc.* **2002**, *124*, 14759−14769. (b) Gearba, R. I.; Lehmann, M.; Levin, J.; Ivanov, D. A.; Koch, M. H. J.; Barbera, J.; Debije, M. G.; Piris, J.; Geerts, Y. H. *Adv. Mater.* **2003**, *15*, 1614−1618. (c) Nguyen, T. Q.; Martel, R.; Avouris, P.; Bushey, M. L.; Brus, L.; Nuckolls, C. *J. Am. Chem. Soc.* **2004**, *126*, 5234−5242. (d) Würthner, F.; Thalacker, C.; Sautter, A. *Adv. Mater.* **1999**, *11*, 754−758.
(7) Hunter, C. A.; Sanders, J. K. M. *J. Am. Chem. Soc.* **1990**, *112*, 5525−5534.
(8) Zhao, D. H.; Moore, J. S. *Chem. Commun.* **2003**, 807−818.
(9) (a) Lin, C. H.; Tour, J. *J. Org. Chem.* **2002**, *67*, 7761−7768. (b) Höger, S.; Bonrad, K.; Rosselli, S.; Ramminger, A. D.; Wagner, T.; Silier, B.; Wiegand, S.; Haussler, W.; Lieser, G.; Scheumann, V. *Macromol. Symp.* **2002**, *177*, 185−191. (c) Zhao, D. H.; Moore, J. S. *J. Org. Chem.* **2002**, *67*, 3548−3554. (d) Tobe, Y.; Utsumi, N.; Kawabata, K.; Nagano, A.; Adachi, K.; Araki, S.; Sonoda, M.; Hirose, K.; Naemura, K. J. *Am. Chem. Soc.* **2002**, *124*, 5350−5364.
(10) (a) Phillips, K. E. S.; Katz, T. J.; Jockusch, S.; Lovinger, A. J.; Turro, N. J. *J. Am. Chem. Soc.* **2001**, *123*, 11899−11907. (b) Nakamura, K.; Okubo, H.; Yamaguchi, M. *Org. Lett.* **2001**, *3*, 1097−1099.

10.1021/ja0430696 CCC: $30.25 **© 2005 American Chemical Society**

mesogens are usually composed of a flat aromatic core substituted in the periphery with flexible, long alkyl chains, which provide solubility and influence the association between the molecules. These aggregates revealed high charge carrier mobilities along the columnar stacking axis, which make them a promising class as active components in electronic devices.[13] Hexa-*peri*-hexabenzocoronene (HBC) exhibits one of the highest intrinsic charge carrier mobilities for a discotic mesogen[14] because of its large aromatic core and strong self-association accordingly into rodlike superstructures. The substitution in the corona of the disk influences the self-association and consequently the thermal properties, solubility and morphology.

Extending the length of the alkyl chain from 3,7-dimethyl-octyl to 3,7,11,15-tetramethyl-hexadecyl resulted in a lowering of the isotropization temperature of about 200 °C.[15] Moreover, we have recently shown that the introduction of sterically demanding, dove-tailed 2-decyl-tetradecyl chains further reduced the temperature of transition to the isotropic state to 46 °C.[16]

For device fabrication, it is important to align the active component in the gap between two electrodes in a way that charges can migrate effectively.[17] Next to adequate electronic properties, the morphology of the material is a crucial property in forming distinct columnar pathways over large domains and thus is closely related to the device performance. Controlling the interactions between the molecules and therefore the self-association by changing the chemical composition is the key factor tailoring the solubility and the thermal properties. The degree of self-aggregation dominates the processing from solution. For solution casting, it is required to deposit pre-aggregated species onto the substrate. It was recently shown that the solution-based zone-casting processing is highly dependent on the solubility and thus on the solution self-aggregation of the single building blocks.[18] Thereby, HBC−C_{12} **1e**, which is known to possess a limited solubility, was successfully aligned by the above-mentioned technique resulting in highly ordered and uniaxially oriented layers. Field-effect transistors (FETs) of **1e** were built exploiting zone-cast films and gave charge carrier mobilities up to 10^{-2} cm^2/Vs.[17b] On the other hand, the optimal processing parameters of discotic materials with an enhanced solubility are more difficult to determine but lead to highly oriented films as well.[19]

Therefore, one major challenge for material science is to tune the self-association of a material because it translates into the processing behavior and furthermore into the performance of a device. Molecules with a pronounced tendency to self-associate are suitable for processing from solution, because the required pre-aggregation is given. Materials with a moderate propensity to aggregate exhibit low isotropization temperatures and become available for processing from the melt.

The self-assembly of HBC-based materials in the bulk and on surfaces has been intensively studied by different techniques such as X-ray diffraction and scanning probe microscopy.[20] The strong tendency of the material to order suggested a detailed study of the self-assembly in relation to the observed morphologies after the processing.

Herein, we describe the synthesis of a homologous series of HBC derivatives with six branched, space-demanding alkyl side chains of different lengths. The solution-phase self-association behavior of this new type of HBC derivative has been compared to the known hexa-*tert*-butyl- **1d** and hexa-dodecyl-hexa-*peri*-hexabenzocoronene **1e**. The aggregation properties influenced by the steric demand of the alkyl chains were analyzed using temperature- and concentration-dependent ^1H NMR, UV/vis, and photoluminescence spectroscopy in different organic solvents. These measurements included the determination of self-association constants and thermodynamic parameters. Furthermore, the morphology formation from solution of the HBC derivatives was investigated, revealing the nucleation and growth of these materials, which is important for the solution processability. Kinetic investigations of the solution casting process were undertaken by varying the evaporation speed of the solvent.

Results

Synthesis. Scheme 1 outlines the previously described synthetic route[21] for C_6-symmetric HBC derivatives. The alkylbromides **3b**,[22] **c** were obtained from the corresponding alcohols **2b**,**c**, whereas 2-ethyl-hexyl-1-bromide **3a** was commercially available. The three branched alkylbromides **3a**−**c** were converted into the corresponding Grignard reagents and subsequently coupled in a Kumada-type reaction with 4,4′-dibromodiphenylacetylene.[23] The alkylated diphenylacetylenes **5a**−**c** were cyclotrimerized to the hexaphenylbenzene-derivatives **6a**−**c** and were planarized with iron(III)chloride to yield the HBC derivatives **1a**−**c** on a multigram scale.

The derivatives **1b**,**c** were the first HBCs highly soluble even in nonpolar solvents, such as pentane or hexane. Moreover, for **1b**,**c**, the long branched chains in the corona of the aromatic disks permitted the purification of the compounds, unlike other known HBCs,[24] by normal preparative column chromatography with hexane as eluent. This efficiently removed all inorganic

(11) Kano, K.; Fukuda, K.; Wakami, H.; Nishiyabu, R.; Pasternack, R. F. *J. Am. Chem. Soc.* **2000**, *122*, 7494−7502.
(12) (a) Farina, R. D.; Swinehar, J.; Halko, D. J. *J. Phys. Chem.* **1972**, *76*, 2343−2348. (b) Terekhov, D. S.; Nolan, K. J. M.; McArthur, C. R.; Leznoff, C. C. *J. Org. Chem.* **1996**, *61*, 3034−3040. (c) Schutte, W. J.; Sluytersrehbach, M.; Sluyters, J. H. *J. Phys. Chem.* **1993**, *97*, 6069−6073. (d) Law, W. F.; Lui, K. M.; Ng, D. K. P. *J. Mater. Chem.* **1997**, *7*, 2063−2067.
(13) (a) Bao, Z. N.; Lovinger, A. J.; Dodabalapur, A. *Adv. Mater.* **1997**, *9*, 42−45. (b) Adam, D.; Schuhmacher, P.; Simmerer, J.; Haussling, L.; Siemensmeyer, K.; Etzbach, K. H.; Ringsdorf, H.; Haarer, D. *Nature* **1994**, *371*, 141−143. (c) Boden, N.; Bushby, R. J.; Clements, J.; Movaghar, B.; Donovan, K. J.; Kreouzis, T. *Phys. Rev. B* **1995**, *52*, 13274−13280.
(14) van de Craats, A. M.; Warman, J. M. *Adv. Mater.* **2001**, *13*, 130−133.
(15) Liu, C. Y.; Fechtenkötter, A.; Watson, M. D.; Müllen, K.; Bard, A. J. *Chem. Mater.* **2003**, *15*, 124−130.
(16) Pisula, W.; Kastler, M.; Wasserfallen, D.; Pakula, T.; Müllen, K. *J. Am. Chem. Soc.* **2004**, *126*, 8074−8075.
(17) (a) van de Craats, A. M.; Stutzmann, N.; Bunk, O.; Nielsen, M. M.; Watson, M.; Müllen, K.; Chanzy, H. D.; Sirringhaus, H.; Friend, R. H. *Adv. Mater.* **2003**, *15*, 495−499. (b) Schmidt-Mende, L.; Fechtenkotter, A.; Müllen, K.; Moons, E.; Friend, R. H.; MacKenzie, J. D. *Science* **2001**, *293*, 1119−1122.
(18) (a) Pisula, W.; Menon, A.; Stepputat, M.; Lieberwirth, L.; Kolb, U.; Tracz, A.; Sirringhaus, H.; Pakula, T.; Müllen, K. *Adv. Mater.*, accepted. (b) Tracz, A.; Jeszka, J. K.; Watson, M. D.; Pisula, W.; Müllen, K.; Pakula, T. *J. Am. Chem. Soc.* **2003**, *125*, 1682−1683.
(19) Pisula, W.; Tomovic, Z.; Stepputat, M.; Kolb, U.; Pakula, T.; Müllen, K., in preparation.
(20) (a) Fischbach, I.; Pakula, T.; Minkin, P.; Fechtenkötter, A.; Müllen, K.; Spiess, H. W.; Saalwachter, K. *J. Phys. Chem. B* **2002**, *106*, 6408−6418. (b) Tchebotareva, N.; Yin, X. M.; Watson, M. D.; Samori, P.; Rabe, J. P.; Müllen, K. *J. Am. Chem. Soc.* **2003**, *125*, 9734−9739. (c) Samori, P.; Yin, X. M.; Tchebotareva, N.; Wang, Z. H.; Pakula, T.; Jäckel, F.; Watson, M. D.; Venturini, A.; Müllen, K.; Rabe, J. P. *J. Am. Chem. Soc.* **2004**, *126*, 3567−3575.
(21) Brand, J. D.; Kübel, C.; Ito, S.; Müllen, K. *Chem. Mater.* **2000**, *12*, 1638−1647.
(22) Hurd, R. N.; Delamater, G.; McElheny, G. C.; Wallingford, V. H.; Turner, R. J. *J. Org. Chem.* **1961**, *26*, 3980−3987.
(23) Mio, M. J.; Kopel, L. C.; Braun, J. B.; Gadzikwa, T. L.; Hull, K. L.; Brisbois, R. G.; Markworth, C. J.; Grieco, P. A. *Org. Lett.* **2002**, *4*, 3199−3202.
(24) Fechtenkötter, A.; Tchebotareva, N.; Watson, M.; Müllen, K. *Tetrahedron* **2001**, *57*, 3769−3783.

Scheme 1. Synthesis of HBC with Bulky, Branched Alkyl Chains of Different Lengths[a]

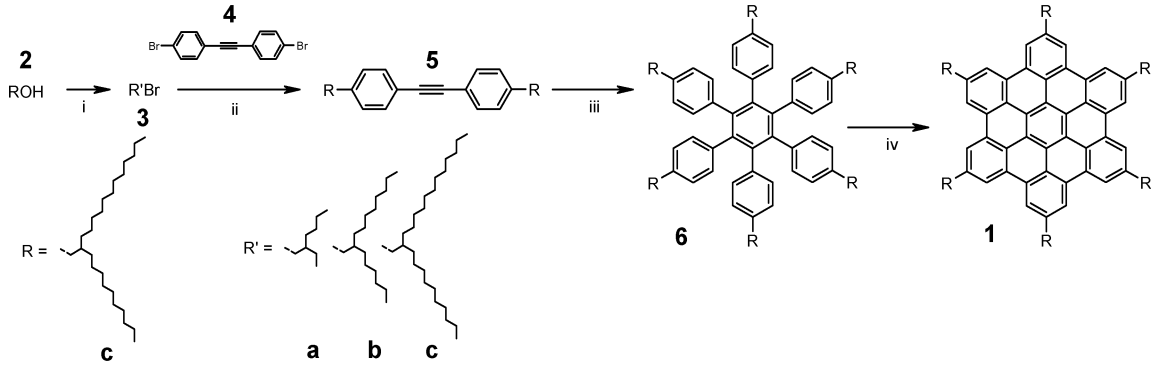

[a] (i) NBS, PPh_3, CH_2Cl_2, 0 °C, 80%; (ii) Mg, THF, $Cl_2Pd(dppf)$, 56−86%; (iii) $Co_2(CO)_8$, dioxane, reflux, 12 h, 75−93%; (iv) $FeCl_3$, CH_3NO_2, CH_2Cl_2, room temperature, 30 min, 75−94%.

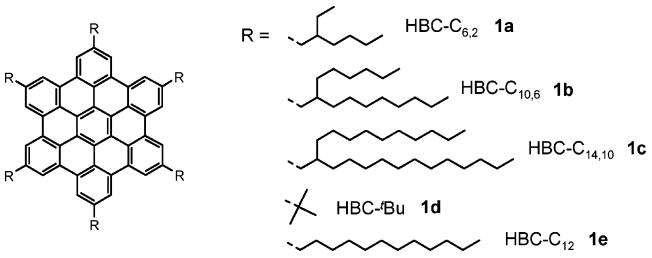

Figure 1. Investigated HBC derivatives.

and organic impurities, obtaining a high level of purity, as indicated by the change of the absorbance and resolution in the UV/vis spectrum of a sample (same concentration) before and after the purification.

The shortest chain **a** did not permit such a purification due to its limited solubilizing effect on the HBC disk. Alternatively, **1a** was repeatedly filtered through a silica plug with hot toluene to remove inorganic impurities from the cyclodehydrogenation step.

Self-Aggregation Behavior. The self-aggregation behavior of the HBC derivatives (Figure 1) was investigated quantitatively by using concentration dependence of the ^{1}H NMR chemical shifts[25] and photophysical measurements. Additionally, these results were compared to those of hexa-*tert*-butyl- **1d** and hexadodecyl-hexa-*peri*-hexabenzocoronene **1e**.[26]

The chemical shift data provide insight not only into the structural arrangement, but furthermore give information about the stacking in solution. Thus, the aromatic resonance of HBC−C_{12} **1e** is strongly dependent on concentration, which is considered as a signature for aromatic stacking.[27] The ring current magnetic anisotropy of an aromatic ring induces a resonance shifting of the nuclei of a molecule, in close vicinity to it.[25] The interacting units are usually in a slightly offset, face-to-face geometry arrangement that leads to an upfield shifting. The chemical shift of the aromatic proton of HBC−C_{12} **1e** in 1,1,2,2-tetrachloroethane-d_2 at 60 °C shifted from 7.9 ppm at a concentration of 1.7×10^{-1} M to 9.0 ppm at 1.0×10^{-6} M, suggesting stacking beyond dimers.[27]

As compared to other systems, such as PAMs, self-association for HBCs occurs in a concentration range, which is at least 1 order of magnitude lower.[28] Recording satisfactory spectra at such low concentrations required high field instrumentation and very long experimental times. With an inverse probe head, spectra of the dilute samples were obtained after about 100 000 scans on a 500 MHz instrument.

In 1,1,2,2-tetrachloroethane-d_2 (Figure 2A), the aromatic resonance for HBC−C_{12} **1e** at 30 °C reached a plateau at a concentration lower than approximately 1×10^{-6} M, which indicated monomeric species. Compounds **1a**−**c** revealed a strong concentration dependence in the ^{1}H NMR spectra occurring at much higher values than in the case of HBC−C_{12} **1e**. Below 1×10^{-5} M, the three HBC derivatives with the branched alkyl chains **1a**−**c** existed as monomers in solution. HBC−$C_{6,2}$ **1a** possessed the lowest solubility among the three dove-tailed HBC samples. In comparison with HBC−$C_{10,6}$ **1b** and HBC−$C_{14,10}$ **1c**, HBC−$C_{6,2}$ **1a** appeared to be more strongly aggregated (chemical shift at higher field at the same concentration). HBC−$C_{10,6}$ **1b** showed the lowest self-association in 1,1,2,2-tetrachloroethane-d_2 at 30 °C, followed by HBC−$C_{14,10}$ **1c** with the longest alkyl substituents, while HBC−^{t}Bu **1d** failed to exhibit association in solution.

Least-squares curve fitting was performed on the concentration-dependent ^{1}H NMR assuming an indefinite self-association process to elucidate the stacking behavior.[25] The association processes were thereby described as consecutive equilibrium states, where monomers were added to the existing aggregate. Additional parameters, such as the chemical shift of the monomer, terminal, and internal units, were required to fit the concentration-dependent NMR data. The commonly used monomer−dimer model, which could be used when association into higher aggregates was negligible, was not suitable to analyze our data. The model of indefinite self-association yielded the best curve fittings for the concentration-dependent ^{1}H NMR data. Table 1 lists the determined association constants. The solution aggregation of HBC−C_{12} **1e** was significantly more pronounced, as already evidenced by a lower solubility. At a concentration of 4.75×10^{-5} M, the average aggregate of HBC−C_{12} **1e** consisted of ca. six disks, but with a broad distribution, while the HBCs with the branched substituents existed as monomers (not shown).

Temperature-dependent ^{1}H NMR spectra were also taken of the aggregating HBC-derivatives **1a**−**c**,**e** at a concentration of

(25) Martin, R. B. *Chem. Rev.* **1996**, *96*, 3043−3064.
(26) Herwig, P.; Kayser, C. W.; Müllen, K.; Spiess, H. W. *Adv. Mater.* **1996**, *8*, 510−513.
(27) Wu, J.; Fechtenkötter, A.; Gauss, J.; Watson, M. D.; Kastler, M.; Fechtenkötter, C.; Wagner, M.; Müllen, K. *J. Am. Chem. Soc.* **2004**, *126*, 11311−11321.
(28) Shetty, A. S.; Zhang, J. S.; Moore, J. S. *J. Am. Chem. Soc.* **1996**, *118*, 1019−1027.

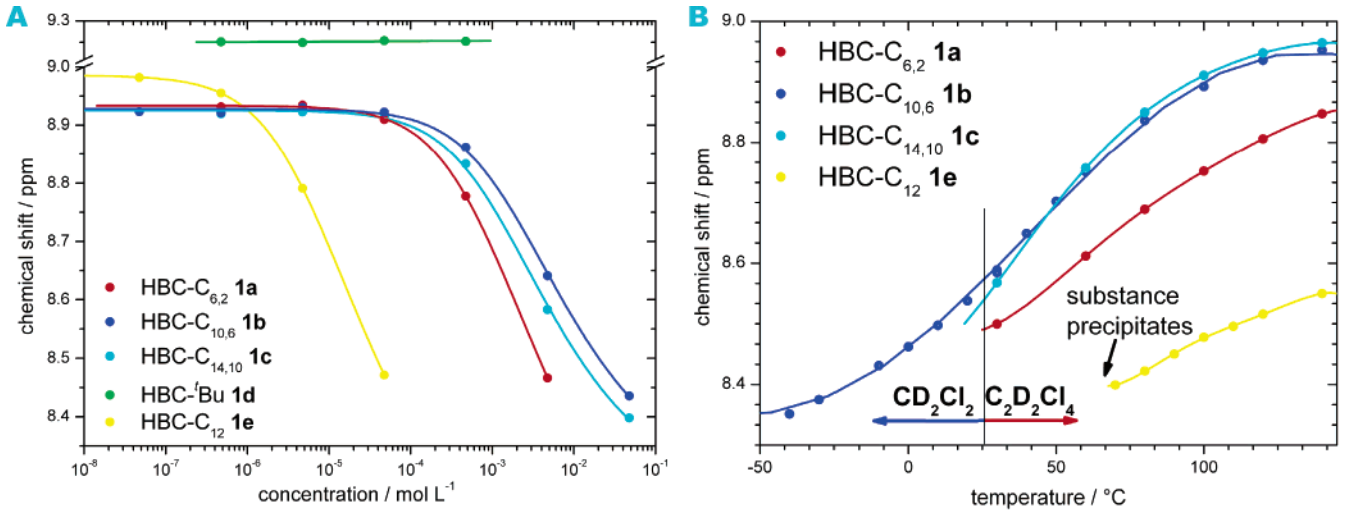

Figure 2. (A) Concentration-dependent ^{1}H NMR chemical shifts, recorded in 1,1,2,2-tetrachloroethan-d_2 (30 °C, 500 MHz), fitted with the indefinite self-association model including next nearest neighbor relations. (B) Temperature-dependent ^{1}H NMR of the investigated HBC derivatives in 1,1,2,2-tetrachloroethane-d_2 and dichloromethane-d_2, respectively, at a concentration of 4.75×10^{-3} M (500 MHz), fitted polynomially (second order).

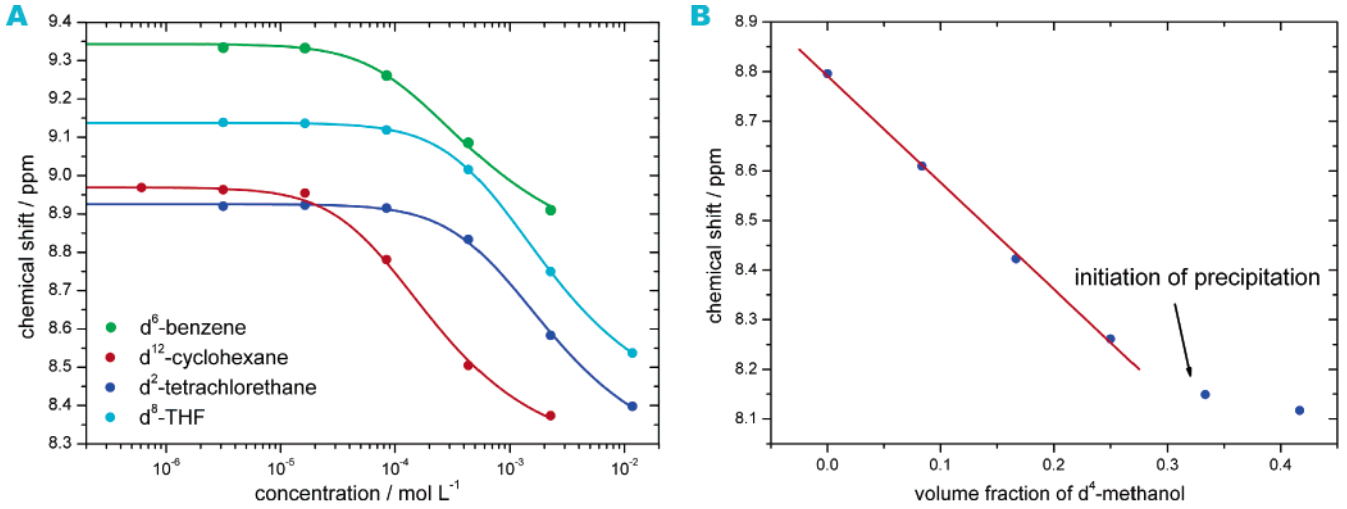

Figure 3. (A) Solvent-dependent aggregation behavior of HBC−C$_{14,10}$ **1c** at 30 °C (500 MHz), fitted with the indefinite self-association model including next nearest neighbor relations. (B) Chemical shift dependence of HBC−C$_{14,10}$ **1c** in a mixture of methanol-d_4 and 1,1,2,2-tetrachloroethane-d_2 with different compositions (concentration: 4.75×10^{-3} M).

Table 1. Association Constants for Self-Aggregation of the Investigated HBC Derivative in 1,1,2,2-Tetrachloroethane-d_2 at 30 °C

compound	K_a/L mol^{-1}
1a	13.4
1b	1.8
1c	2.9
1e	898

Table 2. Association Constants of HBC−C$_{12}$ **1e** and HBC−C$_{14,10}$ **1c** in Different Solvents at 30 °C

NMR solvent	K_a/L mol^{-1} for **1c**	K_a/L mol^{-1} for **1e**
cyclohexane-d_{12}	23.4	not soluble
1,1,2,2-tetrachloroethane-d_2	2.9	900
THF-d_8	3.6	5500[a]
benzene-d_6	420	14 900

[a] Recorded at 40 °C.

4.75×10^{-3} M in 1,1,2,2-tetrachloroethane-d_2. Due to its limited solubility, HBC−C$_{12}$ **1e** could not be measured at a temperature below 70 °C. The aggregation of all investigated structures is also strongly temperature dependent (Figure 2B), whereby HBC−C$_{10,6}$ **1b** aggregated slightly stronger than HBC−C$_{14,10}$ **1c** above 60 °C. Above 130 °C, both derivatives existed exclusively as monomer, because the aromatic resonance reached the value for the monomer. HBC−C$_{12}$ **1e** revealed also the strongest aggregation at high temperatures in relation to the other examples. The chemical shift decreased by lowering the temperature as was observed for HBC−C$_{10,6}$ **1b** dissolved in dichloromethane-d_2.

Figure 3A shows the concentration-dependent ^{1}H NMR fits for HBC−C$_{14,10}$ **1c** in different solvents, and Table 2 summarizes the determined association constants of HBC−C$_{12}$ **1e** and HBC−C$_{14,10}$ **1c**. The aggregation of these two HBC derivatives in 1,1,2,2-tetrachloroethane-d_2 and THF-d_8 was moderate as compared to the values in cyclohexane-d_{12} or benzene-d_6. The self-association in benzene-d_6 was higher than in other solvents, although the chemical compatibility to the aromatic HBCs should be better.

Because the investigated polyaromatic hydrocarbons were insoluble in polar solvents such as acetone-d_6, acetonitrile-d_3, or DMSO-d_6 at the NMR concentration level, the NMR

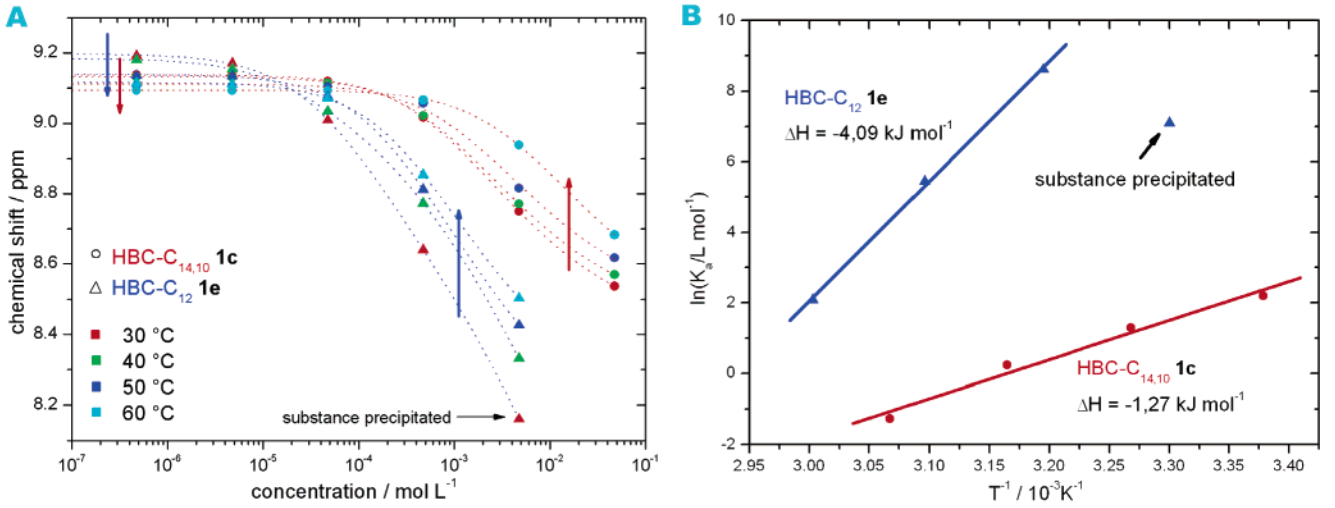

Figure 4. (A) Temperature- and concentration-dependent ^{1}H NMR data of HBC−$C_{14,10}$ **1c** and HBC−C_{12} **1e** in THF-d_8 (500 MHz), fitted with the indefinite self-association model including next nearest neighbor relations. (B) van't Hoff plot of self-association constants K_a for HBC−$C_{14,10}$ **1c** and HBC−C_{12} **1e**.

Table 3. Association Constant K_a and Thermodynamic Parameters for Self-Aggregation of HBC−$C_{14,10}$ **1c** and HBC−C_{12} **1e** in THF-d_8 at 30 °C

compound	K_a/L mol^{-1}	ΔH/kJ mol^{-1}	ΔG/kJ mol^{-1} [a]	ΔS/J mol^{-1} K^{-1}
HBC−$C_{14,10}$ **1c**	3.6	−91.7	−5.82	−290
HBC−C_{12} **1e**	5500	−283	−36.7	−832

[a] At 296 K.

experiments were carried out in a mixed solvent system of 1,1,2,2-tetrachloroethane-d_2 and methanol-d_4, with several different compositions. HBC−$C_{14,10}$ **1c** at a concentration of 4.75 × 10^{-3} M exhibited an increasing tendency to self-aggregate with an increasing portion of the nonsolvent, methanol-d_4, relative to 1,1,2,2-tetrachloroethane-d_2 (Figure 3B). The aromatic resonance of **1c** shifted upfield linearly, until the substance precipitated at a methanol-d_4 volume fraction of 30%. As a control experiment, concentration-dependent measurements in a constant ratio of methanol-d_4 and 1,1,2,2-tetrachloroethane-d_2 were carried out (not shown here). This led to the same results as the previously described experiment, confirming no influence of the chemical shift upon the solvent polarity in the investigated concentration range.

Thermodynamic parameters of the self-association behavior were obtained from determination of association constants at different temperatures in THF-d_8 (Figure 4A). Probably either due to changes of the conformation of the HBC molecules (deviation from planarity) or due to changes of the disk mobility in the solvent cage with increasing temperature, the electronic environment of the protons varied and thus the chemical shifts for the monomeric HBCs at low concentrations decreased with increasing temperature.

The van't Hoff plots for the strongly aggregating HBC−C_{12} **1e** and the less aggregating HBC−$C_{14,10}$ **1c** are shown in Figure 4b, while the thermodynamic data are presented in Table 3. At the lowest temperature and highest concentration, the HBC−C_{12} **1e** sample became cloudy during the measurement. Because the solution NMR measurement detected only aggregates in solution, the determined association constant was too small to fit into the linearized van't Hoff plot.

The electronic spectrum provided a sensitive probe for interactions between molecules within an aggregate.[29] The absorption spectra of HBCs were typical for polycyclic aromatic hydrocarbons, showing the characteristic groups of bands of different extinction coefficients according to the Clar nomenclature: α, *p*, *β*, which correspond to the transitions from the ground-state S_0 into the excited states S_1, S_2, and S_3, respectively. In C_6-symmetric HBCs, the α transition was only weakly allowed and thus difficult to observe, because the transition is geometrically not allowed.[30] According to Kashas law,[31] the photoluminescence spectra exhibit only transitions from S_1 into vibrational levels of S_0.

To gain deeper insight into the self-association behavior, concentration-dependent UV/vis spectra of the feebly self-associating HBC−$C_{14,10}$ **1c** and the strongly aggregating HBC−C_{12} **1e** were recorded, showing only small differences upon concentration changes in the range from 1 × 10^{-4} to 1 × 10^{-7} M (not shown). In the same concentration range, the photoluminescence (PL) and photoluminescence excitation (PLE) spectra revealed a more pronounced effect (Figure 5A). The PL spectra for both compounds were normalized at 480 nm, because this band was only little influenced by concentration. While increasing the concentration, the intensity of the fluorescence bands at 469, 489, and 497 nm decreased for both investigated HBCs. In contrast, the broad band in the region above 500 nm became higher in intensity, indicating the formation of aggregates. The PLE spectra turned out to be a much more sensitive probe for the presence of aggregation. The bands at 345, 360, and 390 nm were strongly dependent on the concentration and lost intensity in concentrated solutions. At high concentrations, a weak, broad band appeared for both investigated HBC derivatives at a wavelength of 407 nm, which could be assigned to an emission from the aggregates. The UV/vis spectra showed an isosbestic point at a wavelength of 398 nm, pointing toward a linear dependence of the two bands at 390 (*p*-band) and 407 nm, respectively (Supporting Information). All PLE spectra in Figure 5A were normalized at the isosbestic point.

The strength of the self-association appeared to be sensitive to solvent effects, as was observed in the above-described ^{1}H

(29) Prince, R. B.; Saven, J. G.; Wolynes, P. G.; Moore, J. S. *J. Am. Chem. Soc.* **1999**, *121*, 3114−3121.
(30) Clar, E. *Polycyclic Hydrocarbons*; Academic: New York, 1964.
(31) Kasha, M. *Discuss. Faraday Soc.* **1950**, 14−19.

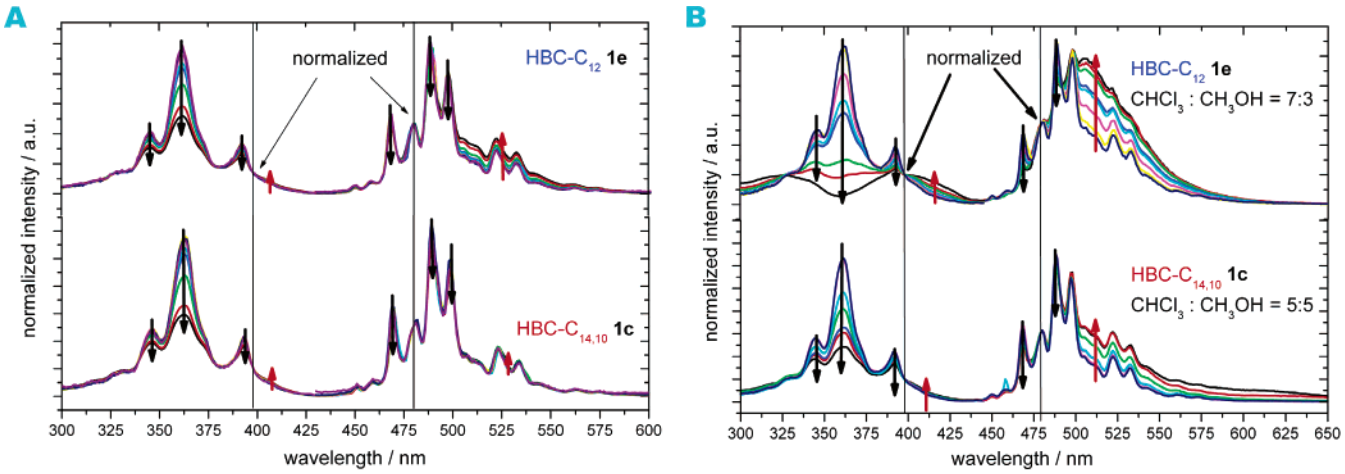

Figure 5. (A) PL and PLE spectra of HBC−$C_{14,10}$ **1c** and HBC−C_{12} **1e** in $CHCl_3$ at concentrations between 1×10^{-4} and 1×10^{-7} M (black to blue); normalized at 480 and 398 nm, respectively. Arrows point in the direction of the high concentration. (B) Concentration-dependent PL and PLE spectra of HBC−C_{12} **1e** and HBC−$C_{14,10}$ **1c** in $CHCl_3$:CH_3OH = 7:3 and 5:5, respectively (concentration from 6×10^{-5} to 4×10^{-7} M, black to blue).

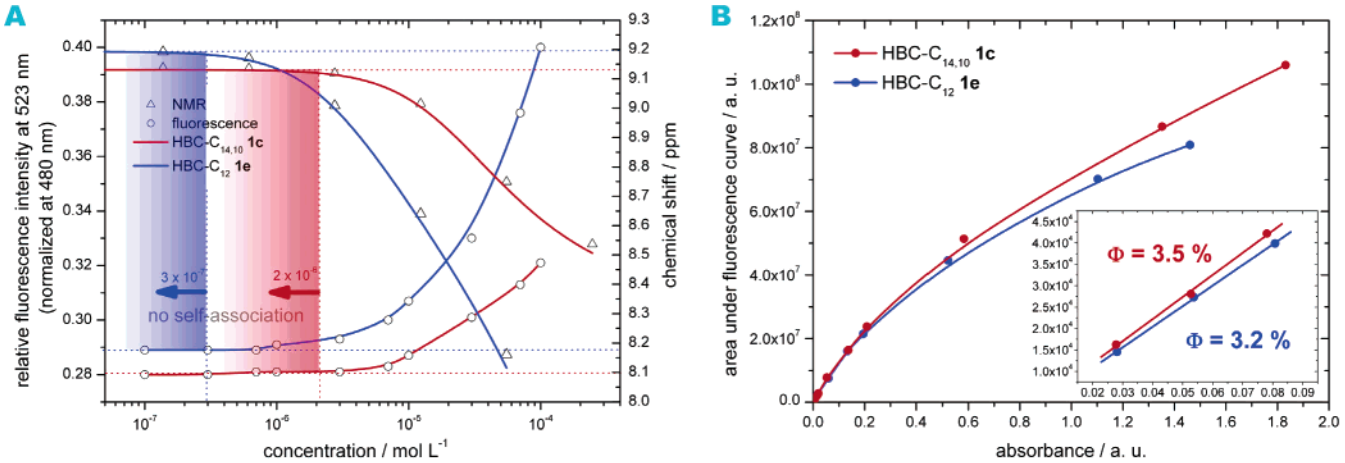

Figure 6. (A) Comparison of PL and ^{1}H NMR (500 MHz) results of HBC−C_{12} **1e** and HBC−$C_{14,10}$ **1c**: PL intensity at 523 nm of the at 480 nm normalized spectra, recorded in THF, and the chemical shift from the ^{1}H NMR, recorded in THF-d_8, are plotted against concentration. (B) Fluorescence yields of HBC−C_{12} **1e** and HBC−$C_{14,10}$ **1c**. Inset: Determination of the fluorescence quantum yields of the two materials in the linear regime at low concentrations (no self-association), all measurements (pathway = 1 cm; 25 °C; absorption and excitation wavelength = 360 nm; integration range = 425−600 nm).

NMR results. Due to the aggregation, a non-Lambert−Beer law behavior was observed for the investigated derivatives. The extinction coefficient decreased slightly, when the concentration was increased. A more pronounced effect was observed, when the polarity of the solvent was changed.

In the case of HBC−$C_{14,10}$ **1c**, the maximum absorption in the UV/vis spectrum (β-band) shifted hypsochromically from 362 to 358 nm as either the content of methanol or the concentration increased, whereas the same band for HBC−C_{12} **1e** did not shift at all (Supporting Information). The photoluminescence spectra of HBC−$C_{14,10}$ **1c** and HBC−C_{12} **1e**, recorded concentration dependent (1×10^{-4} to 1×10^{-7} M) in a mixture of chloroform and methanol with a ratio of 7:3 and 5:5, respectively, exhibited a dramatic change with respect to the polarity of the solvent (Figure 5B). The main band in the PLE for HBC−C_{12} **1e** disappeared completely, whereas the band at 415 nm intensified. The changes in the PL and PLE spectra for HBC−$C_{14,10}$ **1c** were identical to the concentration-dependent measurements in chloroform, where the region above 500 nm pointed toward self-association.

Plotting the change of the relative intensity of the band at, for example, 523 nm from the normalized photoluminescence spectrum versus the concentration gave a curve that was comparable to the concentration-dependent ^{1}H NMR plot (Figure 6A). At a nominal concentration of 3×10^{-7} M for HBC−C_{12} **1e** and 2×10^{-4} M for HBC−$C_{14,10}$ **1c**, the concentration-dependent plots from both measurements leveled out, indicating the presence of only the monomeric species in solution. Plotting the values for absorbance at 360 nm determined by UV/vis spectroscopy versus the area under the corresponding PL curve (excitation at 360 nm) yielded two different curves for HBC−C_{12} **1e** and HBC−$C_{14,10}$ **1c** (Figure 6B). The inner filter effect became dominant at high absorbances, making an interpretation difficult. On the other hand, because both derivatives possess almost identical extinction coefficients at low concentrations, the difference between the two plots at large absorbances was remarkable. For HBC−C_{12} **1e**, the extinction coefficient was far more dependent on the concentration, and furthermore the fluorescence as compared to HBC−$C_{14,10}$ **1c** was strongly quenched, which could be attributed to the higher self-association of HBC−C_{12} **1e**.

The inset in Figure 6B suggests only a slight difference in the fluorescence quantum yield between HBC−C_{12} **1e** (3.2%) and HBC−$C_{14,10}$ **1c** (3.5%), proving the similar elec-

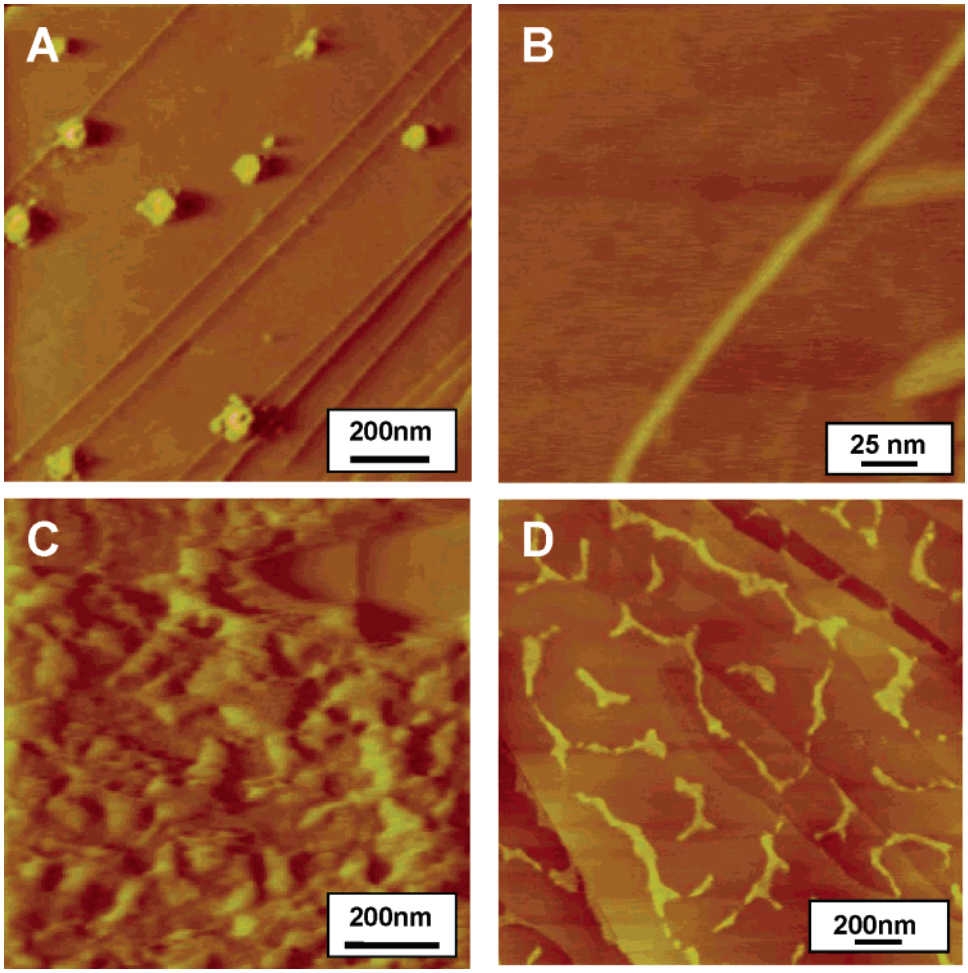

Figure 7. AFM images in tapping made on HOPG surface of spin-coated films HBC−$C_{14,10}$ **1c** from (A) a 10^{-7} M THF solution and (C) a 10^{-4} M solution; HBC−C_{12} **1e** from (B) a 10^{-7} M THF solution and (D) a 10^{-4} M solution.

tronic behavior of the two substances in the absence of self-association.

Temperature-dependent UV/vis and PL spectroscopy was conducted on samples of differing concentration, exhibiting only very small effects with temperature changes.

After having gained information about the self-association of the HBC derivatives in solution, it was important to explore how the solution behavior translates into the solution processing, which is a key step in implementing the materials successfully into electronic devices based on organic materials. To investigate the effect of self-association at the interface between solvent and substrate onto the film morphology[32] of the HBC derivatives, the organization from solution was investigated by the AFM technique. Therefore, the samples were first prepared by spin-coating at room temperature on HOPG surfaces.

When HBC−$C_{14,10}$ **1c** was spin-cast from a 10^{-4} M THF solution, the freshly cleaved graphite surface was covered by an inhomogeneous ∼100 nm thick film that showed no nanoscopic order (Figure 7C), whereas the film from HBC−C_{12} **1e** prepared under the same conditions exhibited a more pronounced anisotropy in the structure, such as fibrous features (Figure 7D). When decreasing the concentration down to 10^{-7} M, in the case of HBC−$C_{14,10}$ **1c** single 60−80 nm wide blobs with a height of ca. 3 nm appeared, which were randomly distributed over the surface (Figure 7A). From a solvent mixture of methanol and chloroform (1:1) at the same concentration, single flat pancake-shaped features with a constant thickness of ca. 2.5 nm were formed (not shown).

Single long nanofibers were found from a 10^{-7} M solution of HBC−C_{12} **1e** in THF, which were 1.2 nm high and ca. 20 nm wide, exceeding even several hundreds of nanometers in length (Figure 7B). These fibers seemed to consist of a monomolecular layer with several columns lying parallel along the fiber axis, whereby the molecules were arranged edge-on.

The morphology of a drop-cast film (10^{-4} M in toluene) of HBC−C_{12} **1e** (Figure 8) consisted of several hundred micrometers long, birefringent microfibers. Their dimensions slightly changed with different solvents. By casting from toluene, longer, but thinner, microfibers were observed in comparison to the films prepared from THF or other solvents with lower evaporation temperatures. In all cases, the morphology was uniform within the drop-cast film, whereby the columnar alignment coincided with the microfiber axis as it was previously proven.[33] Indeed, the spin-coated HBC−C_{12} **1e** films revealed highly oriented columnar domains as visualized by transmission

(32) (a) Nguyen, T. Q.; Bushey, M. L.; Brus, L. E.; Nuckolls, C. *J. Am. Chem. Soc.* **2002**, *124*, 15051−15054. (b) Klok, H. A.; Jolliffe, K. A.; Schauer, C. L.; Prins, L. J.; Spatz, J. P.; Moller, M.; Timmerman, P.; Reinhoudt, D. N. *J. Am. Chem. Soc.* **1999**, *121*, 7154−7155. (c) Jonkheijm, P.; Hoeben, F. J. M.; Kleppinger, R.; van Herrikhuyzen, J.; Schenning, A.; Meijer, E. W. *J. Am. Chem. Soc.* **2003**, *125*, 15941−15949.

(33) Kübel, C. Dissertation, Johannes Gutenberg Universität, 1998.

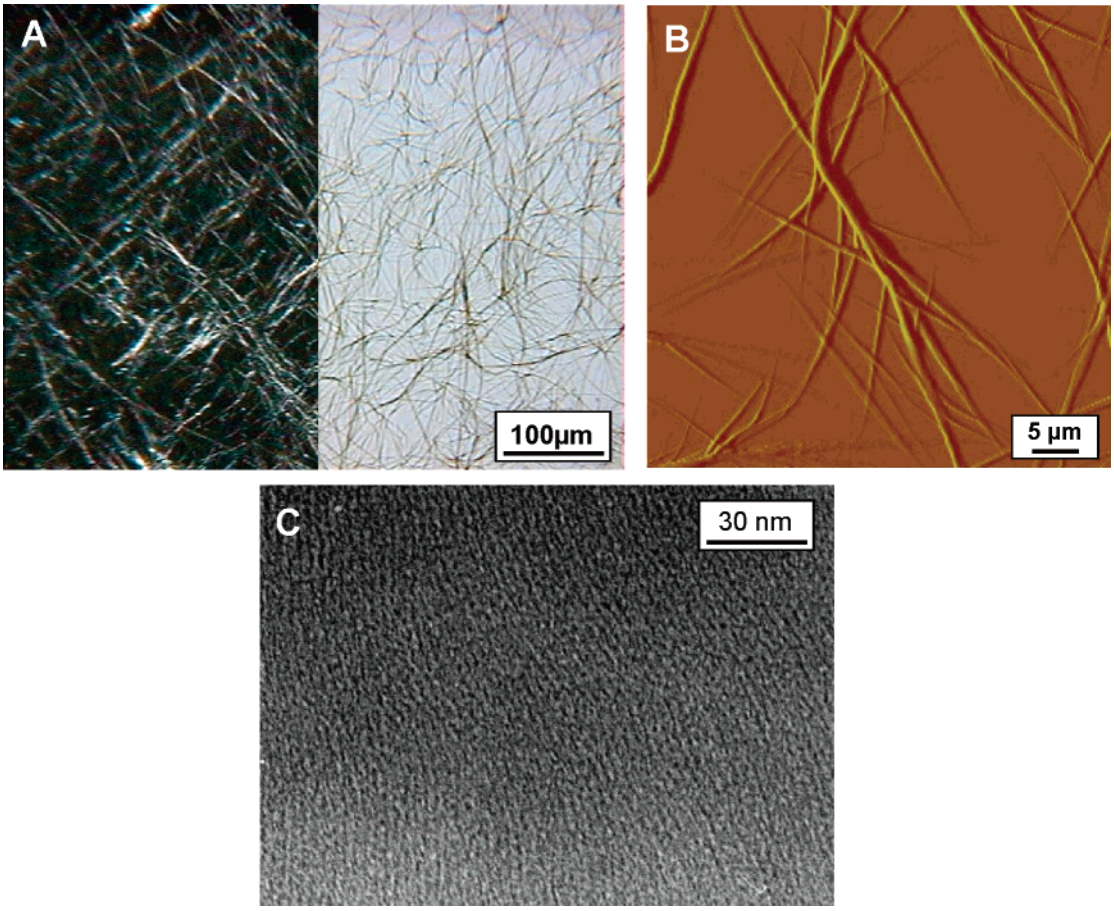

Figure 8. (A) POM image of drop-cast HBC−C_{12} **1e** from a 10^{-4} M toluene solution (right with and left without cross-polarizer); (B) AFM topography of the microfiber morphology (tapping mode); (C) TEM image of a spin coated HBC−C_{12} **1e** film (10^{-4} M toluene).

electron microscopy (TEM) (Figure 8C). This tendency to create highly anisotropic structures was even observed within a polymer matrix.[34]

On the other hand, drop-cast HBC−$C_{14,10}$ **1c** and HBC−$C_{10,6}$ **1b** films from 10^{-4} M THF solutions were completely amorphous. By using toluene as solvent, the film morphology changed slightly, revealing birefringent parts that appeared at the rim of the drop-cast films where most of the material was deposited.

The drop-cast film of HBC−$C_{6,2}$ **1a** (Figure 9) prepared from a 10^{-4} M THF solution also did not show any birefringence in polarized light, but small particles precipitated randomly from the solution. When the same material was processed from toluene with an identical concentration, short crystalline needles appeared at the rim of the film (Figure 9C). These structures were highly birefringent and were mainly oriented in the direction of the drop evaporation, whereas the interior of the film revealed the same, but shorter, structures (Figure 9A). By using a comparable solvent with respect to the association such as xylene, which possesses a significantly higher evaporation temperature, the length of these crystalline needles within the film interior increased considerably (Figure 9B). Finally, when a saturated toluene solution of HBC−$C_{6,2}$ **1a** was slowly evaporated from a small vessel, centimeter-long, crystalline fibers were obtained on the bottom of the vessel (Figure 9D).

Due to this extraordinary nucleation and growth of such large fibers in solution, a dipping experiment was performed to align these structures uniaxially as shown in Figure 10A. At a concentration of 10^{-1} M in toluene and a low moving velocity of the support, a homogeneous film was acquired with indeed oriented microfibers (Figure 10C,D). Moreover, these fibers consisted of uniaxially aligned HBC columns as the 2D WAXS pattern indicated (Figure 10B).

Discussion

Because the investigated HBC derivatives did not possess any functional group, which were capable of forming, for example, hydrogen bonds, one assumed a face-to-face π-stacking of the aromatic cores, based on the concentration dependence of the aromatic resonance in the NMR. The influence of the ring current from neighboring molecules caused the shift of the aromatic protons, decreasing with increasing distance from the core.[9d] The α-carbon of the aliphatic side chain exhibited a much smaller concentration dependence, whereas the chemical shift of the next carbon in the chain was almost independent of concentration.

The observed self-association equilibria for the hexa-alkylated HBCs were fast on the time scale of the NMR experiment, leading to only one broadened, averaged peak for all aggregates. Recently, we described oligophenylene dendronized HBC, which enhanced the attractive interactions between the molecules.[27] There, the equilibrium kinetics of the dendronized HBC

(34) Tracz, A.; Wostek, D.; Kucinska, I.; Jeszka, J. K.; Watson, M.; Müllen, K.; Pakula, T. In *NATO Advanced Study Institute Series*; Graja, A., Buła, R., Kajzar, F., Eds.; Kluwer: Dordrecht, 2002; p 315.

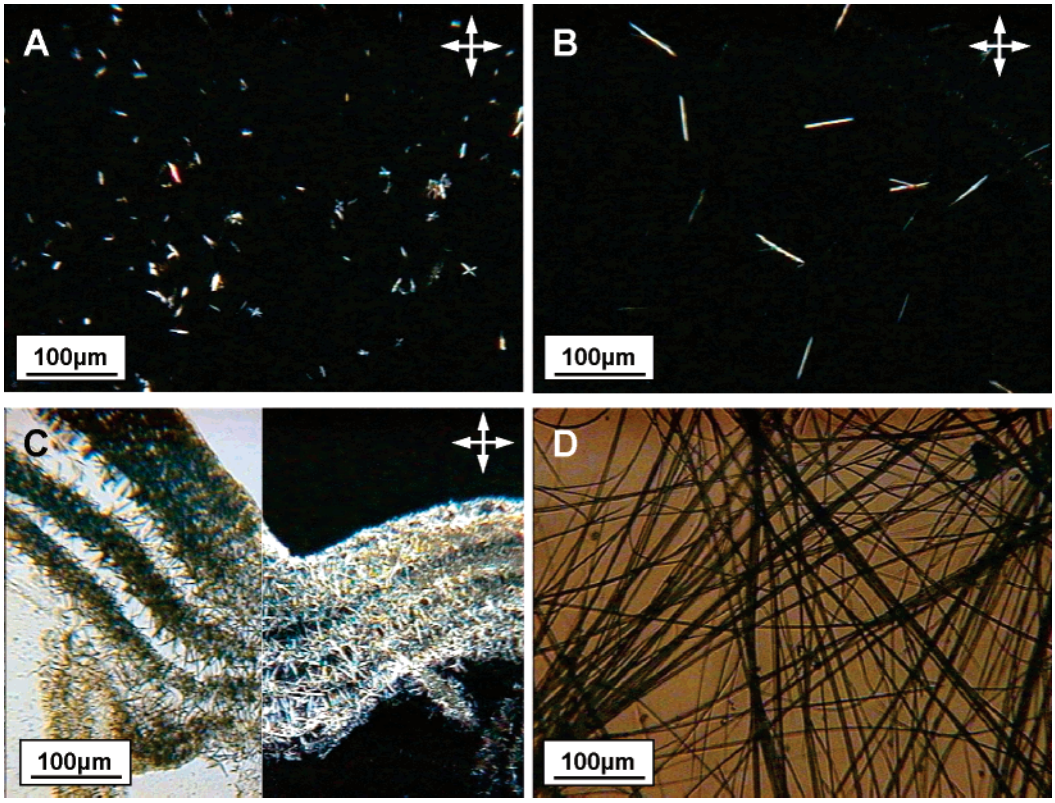

Figure 9. POM of HBC−$C_{6,2}$ **1a** drop-cast from (A) toluene and (B) xylene both at a concentration of 10^{-4} M, (C) optical image of the rim of the drop-cast film prepared in (a) (left without and right with cross-polarizer), and (D) optical image obtained after evaporation of a HBC−$C_{6,2}$ solution with a concentration close to the saturation.

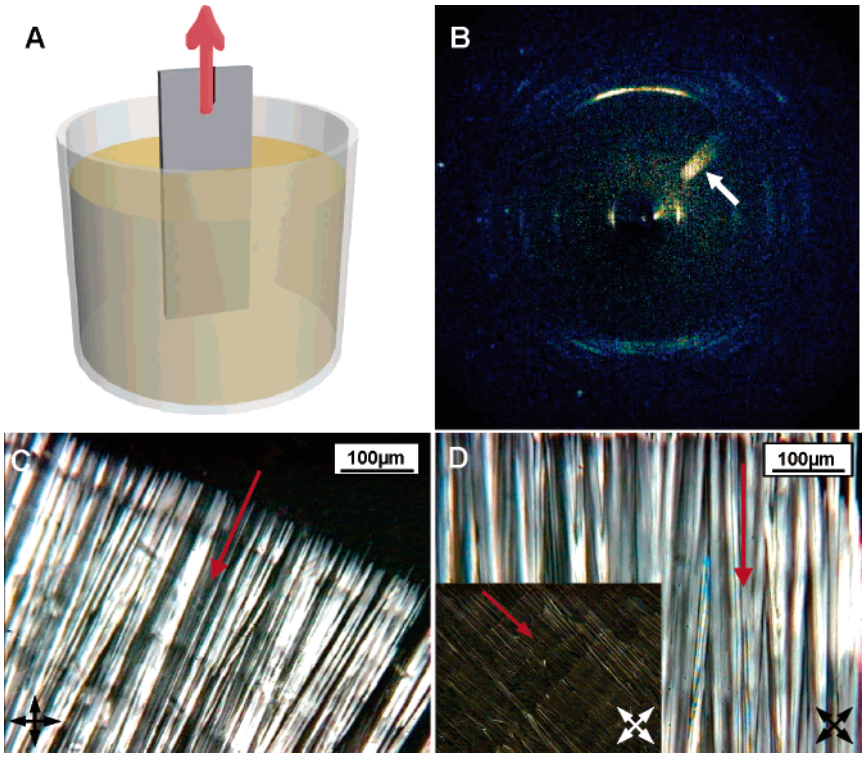

Figure 10. (A) Setup for the dipping experiment of HBC−$C_{6,2}$ **1a**; at the deposition zone, a meniscus is formed at which the material crystallized onto the moving support; (B) 2D WAXS pattern of the oriented HBC−$C_{6,2}$ **1a** film (arrow indicates an artifact); (C) POM of the nucleation site, at which the structures begin to grow in the moving direction of the support; (D) POM of the interior of the film revealing a uniaxial orientation of the microfibers.

was much slower as compared to the time scale of the NMR, as indicated by the observation of distinct aromatic resonances for monomeric and dimeric species.

The self-association behavior of the HBCs with branched alkyl substituents occurred in a different concentration range as compared to the parent HBC−C_{12} **1e**. Bulky *tert*-butyl-groups

in the HBC periphery suppressed aggregation completely and possessed a low solubilizing effect, which has already been confirmed by UV/vis and time-resolved fluorescence measurements.[35] It is presumed that substituents, exhibiting a large steric demand in the close vicinity of the disk, prevent the molecules from closely approaching each other, thereby hindering π-stacking.[28] This observation confirmed the notion that HBCs were cofacially stacked. In our study, HBC−C_{12} **1e** showed the strongest aggregation in the concentration range from $\sim 10^{-4}$ to $\sim 10^{-7}$ M accompanied by the lowest solubility. Depending on the temperature and the nature of the solvent, the HBC existed on average as monomer at a concentration at ca. 10^{-7} M, which was at least an order of magnitude lower than that reported for the other π-systems.[12b] The solubilizing dodecyl chains possessed only a small steric demand in the periphery of the aromatic disk, which allowed the molecules to approach easily, resulting in a high association constant. The three new HBC derivatives, which carried space-filling alkyl, dove-tailed substituents, self-associate only at much higher concentrations, showing substantially smaller association constants as compared to HBC−C_{12} **1e**. The steric hindrance induced by the side chains perturbed the disks from approaching one another.[36] Comparing HBC−$C_{6,2}$ **1a** to HBC−$C_{10,6}$ **1b**, the length of the side chains increased and led to a diminished self-association. Further extension to HBC−$C_{14,10}$ **1c** did not reduce the aggregation in solution at room temperature because now the interactions between the chains became significant. The attractive interactions, initiated by the long chains, enhanced the self-association slightly, resulting in a higher association for HBC−$C_{14,10}$ **1c** as compared to the derivative **1b**. At higher temperatures, the van der Waals forces decreased and HBC−$C_{14,10}$ **1c** exhibited as expected the lowest self-association among the investigated HBCs. Thus, the steric hindrance modulated the strength of the self-association in solution, and temperature affected the aggregation size additionally as can be seen from Figure 2b.

Furthermore, the self-association was strongly dependent on the nature of the solvent.[37] The association constant for HBC−$C_{14,10}$ **1c** in cyclohexane-d_{12} as solvent was about 10 times higher than those in THF-d_8 and 1,1,2,2-tetrachloroethane-d_2, which could be attributed to the solvophobic effect. It was assumed that aromatic solvents suppress π-stacking between aromatic solutes because such interactions between the solute and solvent would have prevailed over those between solutes. On the contrary, it was observed that HBCs self-associate stronger in benzene-d_6, which was confirmed in previous studies for macrocycles such as PAMs.[9d]

Addition of methanol to the solution of HBCs enhanced the solvophobic interactions, leading to stronger aromatic stacking.[38] At the same concentration, the resonance of the aromatic HBC protons shifted with increasing methanol content upfield, indicating a stronger self-association. Additionally, the concentration-dependent UV/vis (Supporting Information) and photoluminescence measurements in a constant mixture of chloroform and the nonsolvent methanol revealed the existence of aggregates. The presence of an isosbestic point at a wavelength of 398 nm revealed a linear dependence between the monomer absorption and the absorption of aggregates. In the PL, the broad, less resolved, concentration-dependent bands above 500 nm pointed toward the existence of aggregates. The photophysical changes in the case of HBC−$C_{14,10}$ **1c** were less pronounced due to the reduced self-association in solution or the hindered electronic coupling between neighboring molecules. The hypsochromic shift in the case of HBC−$C_{14,10}$ **1c**, which was not observed for the parent HBC−C_{12} **1e**, suggested a different electronic coupling between the aromatic disks and thus a different geometrical arrangement in the aggregated stacks. This is possibly due to a different geometry in the aggregate caused by the large steric demand of the substituents in the corona.

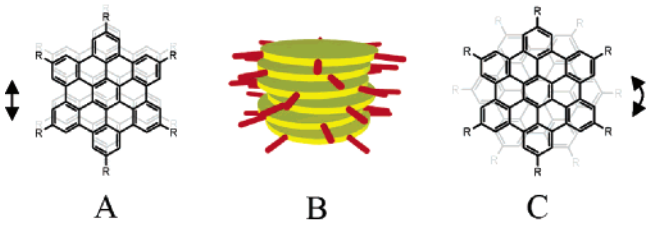

Figure 11. Stacking motif for neighboring HBCs: (A) lateral displacement, (B) schematic structure of an aggregate with rotational and translational offsets in the lateral direction, and (C) rotational offset along the stacking axis.

Quantum mechanical calculations including electron configuration interactions were performed for a better understanding of the spectral changes in the UV/vis of both investigated compounds (Software: Hypercube, Inc., HyperChem 6.0 for Windows). After the optimization of the HBC geometry with an ab initio calculation (basis set: 6-31G*), PM3 calculations (20 occupied and 20 unoccupied orbitals for electron configuration) were applied to dimeric HBC stacks with a distance between the cores of 3.6 Å, as was experimentally determined by powder X-ray diffractometry. Translation and lateral rotation of the disks with respect to each other, which is energetically favored[39] (Figure 11), influenced significantly the calculated electronic spectra. Therefore, it is reasonable to assume the existence of different averaged stacking motifs for the two HBCs. On the basis of the performed calculations, it is not possible to identify specific geometrical arrangements of the HBCs in solution.

For all investigated HBCs, the fluorescence quantum yields were in the same range, but the behavior of HBC−C_{12} **1e** and HBC−$C_{14,10}$ **1c** differed significantly at high concentrations, indicating either different mechanisms of fluorescence quenching due to different geometries of the molecules with respect to each other or a stronger self-association behavior at high concentration, which was supported by the ^{1}H NMR solution measurements.

NMR and fluorescence spectroscopy allowed the independent determination of the critical concentrations for self-association of HBC−$C_{14,10}$ **1c** and HBC−C_{12} **1e**.

The thermodynamic parameters derived from the temperature- and concentration-dependent NMR data suggested that there was an enthalpy gain accompanied by an entropy punishment during the aggregation process, which was also observed for PAMs. In contrast to the PAMs, which have a much smaller π-area,

(35) Biasutti, M. A.; Rommens, J.; Vaes, A.; De Feyter, S.; De Schryver, F. D.; Herwig, P.; Müllen, K. *Bull. Soc. Chim. Belg.* **1997**, *106*, 659−664.
(36) Luz, Z.; Poupko, R.; Wachtel, E. J.; Zimmermann, H.; Bader, V. *Mol. Cryst. Liq. Cryst.* **2003**, *397*, 367−377.
(37) Höger, S.; Bonrad, K.; Mourran, A.; Beginn, U.; Möller, M. *J. Am. Chem. Soc.* **2001**, *123*, 5651−5659.
(38) Lahiri, S.; Thompson, J. L.; Moore, J. S. *J. Am. Chem. Soc.* **2000**, *122*, 11315−11319.
(39) Gauss, J.; Ochsenfeld, C., in preparation.

the association enthalpy for the investigated HBCs was much higher.[28] The Gibbs free energies for HBC−C_{12} **1e** and HBC−$C_{14,10}$ **1c** reflect the difference in association between the two substances.

The investigation of the film morphology obtained through solution casting revealed additional information about the solution behavior of the HBC derivatives. It has been found that in addition to the thermodynamical aspect the organization from solution is also dominated by kinetics. This has been impressively demonstrated in the case of HBC−$C_{6,2}$ **1a**, which was prepared from different solvents with different evaporation rates.

Comparing the films of HBC−$C_{6,2}$ **1a** which were drop-cast from solvents such as toluene and xylene, in which the self-association is known to be very similar, one observed larger micro-objects in the case of the higher boiling xylene. The morphology of a film obtained from THF differed significantly, because only an amorphous structure was obtained. In the latter case, it should be noted that the degree of self-association is smaller.

Nevertheless, the evaporation time of the solvent in the casting process influenced significantly the macroscopic self-organization on the substrate. A slow evaporating solvent such as xylene allowed the formation of large anisotropic objects, whereas a solvent with a lower boiling point did not give enough time to exhibit a similar organization. The role of the kinetics in the case of HBC−$C_{6,2}$ **1a** is more pronounced as compared to that of HBC−C_{12} **1e**. This effect can be explained by the steric requirement induced by the dove-tailed alkyl substituents, which hampered the disks from approaching one another. Therefore, the self-assembly of these molecules occurs on a relatively large time scale. This stands in contrast to HBC−C_{12} **1e**, which revealed homogeneously distributed micro-ribbons over the drop-cast film independent of the used solvent. These extraordinary structures resulted, on one hand, from the strong self-association tendency and, on the other hand, from the low steric demand of the attached alkyl chains.

Consequently, HBC−C_{12} **1e** was successfully processed by the zone-casting technique into highly ordered surface layers, supported by the pronounced size of the pre-aggregates, which existed already before the deposition from solution. In contrast, it is difficult to zone-cast HBC−$C_{6,2}$ **1a** due to its slow self-aggregation and the necessity of using high concentrations to reach a sufficient pre-aggregation in solution. On the other hand, adequate processing conditions during a dipping experiment (higher concentrations and low solvent evaporation rates) allowed an uniaxial orientation into surface layers. This solution processing promises a successful implementation of the material in a FET device.

Due to the increase of the peripheral steric demand of the longer dove-tailed side chains, both compounds HBC−$C_{14,10}$ **1c** and HBC−$C_{10,6}$ **1b** showed a limited tendency to create anisotropic structures from solution. No enhancement in the self-organization onto the surface was observed, even though larger pre-aggregates were observed by the addition of methanol. Both HBC derivatives only formed small domains after the deposition, because the association rate decreased extremely as compared to HBC−$C_{6,2}$ **1a**.

The small difference of the hydrodynamic radius between the aggregates and the monomeric species and the polydispersity of the distribution made scattering methods such as dynamic light scattering or X-ray scattering tenuous. Vapor pressure osmometry (VPO) and dynamic light scattering experiments did not provide interpretable results, due to low solubility and small contrast in the tested solvents.

Conclusion

We have described the synthesis of three novel HBC derivatives with sterically demanding alkyl substituents. The complementary higher solubility enabled a more straightforward purification. The materials showed a reduced self-association behavior in solution, as compared to the parent HBC−C_{12} **1e**, which exhibited, due to the large π-area and unhindered stacking, one of the highest self-association constants based on π-stacking. The steric requirement of the substituents allowed tuning of the self-association in solution, which is a key step for materials science in designing building blocks for self-assembly, where the property of the single molecule translates into the supramolecular architecture. The self-association was an enthalpically driven process, which was, as expected, entropically not favored.

In polar solvents, the association of HBCs was enhanced due to the solvophobic effect. Astonishingly, the association in benzene, as a potentially HBC compatible solvent, was very high, what could not be explained until now. NMR and PL spectroscopy were both suitable to detect the critical concentration for aggregation.

Morphology studies revealed that both the thermodynamical properties and the kinetic aspects are important during self-aggregation in solution. These conclusions should elucidate whether the solution association propensity can be translated to the bulk behavior and thus used for the processing of the material and device fabrication. This result is of fundamental importance in predicting the bulk properties (e.g., thermal behavior, solubility) of new materials prior to the synthesis and thus designing promising candidates for a successful application in organic devices.

Acknowledgment. This work has been financially supported by the Zentrum für Multifunktionelle Werkstoffe und Miniaturisierte Funktionseinheiten (BMBF 03N 6500), the Deutsche Forschungsgemeinschaft (Schwerpunktprogramm Organische Feldeffekt-Transistoren), as the EU projects DISCEL (G5RD-CT-2000-00321), NAIMO (NMP4-CT-2004-500355), and MAC-Mes (GRD2-2000-30242). M.K. thanks the "Fonds der Chemischen Industrie" and the "Bundesministerium für Bildung und Forschung" for financial support. We thank Dr. M. Wagner and S. Spang for conducting high-resolution, solution NMR experiments, J. Schnee for recording photoluminescence spectra, M. Harding from the "Johannes Gutenberg Universität Mainz" for compiling and debugging the fitting algorithm, and T. Julius for graphical support.

Supporting Information Available: Experimental procedures, characterization for the described compounds, and additional UV/vis spectra. This material is available free of charge via the Internet at http://pubs.acs.org.

JA0430696